Computational Modelling of Concrete and Concrete Structures –
Meschke, Pichler & Rots (Eds)
© 2026 The Author(s), ISBN: 978-1-041-11408-6

Non-proportional sequentially-linear analysis for masonry structures: capturing combined foundation settlement and pushover loads

Z. Dai, P.A. Korswagen and J.G. Rots
Department of Materials, Mechanics, Management & Design, Faculty of Civil Engineering and Geosciences, Delft University of Technology, Delft, The Netherlands

ABSTRACT: Unreinforced masonry (URM) walls are highly sensitive to non-proportional loading histories, particularly when foundation settlement precedes lateral loading. In such cases, pre-damage induced by settlement can significantly affect the subsequent structural response and cannot be adequately represented using proportional loading assumptions or equivalent reduction factors.

A Total Sequentially Linear Analysis (Total SLA) framework is developed to investigate the combined effects of boundary conditions, geometry, and settlement-induced pre-damage on the pushover response of URM walls. The numerical model represents masonry units as linear elastic continua and concentrates nonlinearity within zero-thickness interface elements governed by discrete damage modes. Settlement and pushover are applied sequentially within a unified event-driven formulation, allowing damage states to be inherited across loading stages.

The results show that the initial elastic response is largely insensitive to the top boundary conditions, whereas significant differences emerge during the softening phase. Fixed-top configurations exhibit a more gradual degradation of stiffness. Cantilever and free-top conditions, in contrast, show sliding-dominated behavior. Settlement causes irreversible damage, reducing both stiffness and peak capacity during subsequent pushover loading. The effects are amplified in walls with openings. These results demonstrate that neglecting load-path dependency may lead to inaccurate predictions of stiffness degradation and peak capacity in URM walls.

1 INTRODUCTION

Unreinforced masonry (URM) structures represent a large portion of the built heritage in Europe. These structures are increasingly vulnerable to cumulative damage induced by anthropogenic hazards, such as ground settlement due to gas extraction or tunneling (Giardina et al. 2012, Amorosi et al. 2014), followed by seismic events. The structural response under such conditions is strongly path-dependent (Lagomarsino et al. 2013, Korswagen et al. 2022). Cracks formed during the settlement phase modify the stiffness distribution and alter the failure mechanisms of the structure. As a result, the pushover capacity may be significantly reduced. A reliable prediction of this behavior requires a numerical approach that can properly account for non-proportional and multi-stage loading histories.

Numerical modeling of URM structures is challenging due to its quasi-brittle behavior. Continuum models combined with implicit solvers and Newton-Raphson iterative schemes often experience convergence difficulties (Massart et al. 2007, Pulatsu et al. 2020, Koutras & Shing 2021). In particular, softening behavior and snap-back responses associated with crack propagation are difficult to capture in a stable manner. Explicit dynamic solvers can overcome convergence issues, but they are computationally expensive and highly sensitive to damping assumptions when applied to quasi-static problems.

Sequentially Linear Analysis (SLA) has therefore been proposed as a robust alternative to conventional nonlinear solution strategies (Rots & Invernizzi 2004). In SLA, the nonlinear softening behavior is approximated by a sequence of linear analyses with positive stiffness. This approach avoids iterative procedures and guarantees convergence at each load increment. However, classical SLA formulations are limited to proportional loading conditions. Extending the method to non-proportional and sequential loading paths remains an open challenge (DeJong et al. 2008, Pari et al. 2018).

In this paper, a phased total Sequentially Linear Analysis framework is proposed to simulate the damage evolution of URM walls subjected to sequential settlement and pushover loading. The loading process is divided into distinct phases, including overburden application, settlement, and

DOI: 10.1201/9781003660026-55

lateral pushover, during which the internal force distribution evolves significantly. To address this, a non-proportional loading solver is developed and implemented in a modular MATLAB environment.

2 NUMERICAL METHODOLOGY

2.1 *Total formulation for non-proportional loading*

The numerical analyses are carried out using a Total Sequentially Linear Analysis (Total SLA) formulation developed to handle non-proportional loading histories. Unlike incremental approaches, the Total formulation enforces global equilibrium at each discrete damage event. As a result, the structure is always in a fully balanced state, without residual imbalance carried over from previous steps.

At any stage of the analysis, the total displacement field ($\boldsymbol{u}_{\text{total}}$) is decomposed into a constant component inherited from previous loading phases and a variable component associated with the current loading direction:

$$\boldsymbol{u}_{\text{total}} = \boldsymbol{u}_{\text{const}} + \lambda \boldsymbol{u}_{\text{var}}\,, \tag{1}$$

where $\boldsymbol{u}_{\text{const}}$ represents the displacement state fixed at the end of the previous phase (e.g. overburden loading or foundation settlement), $\boldsymbol{u}_{\text{var}}$ stands for the displacement shape vector for the current loading phase, and λ is a scalar load factor controlling the progression toward the next damage event.

Assuming linear elastic behavior between two consecutive damage events, the corresponding stress field can be expressed in an analogous form:

$$\boldsymbol{\sigma}_{\text{total}} = \boldsymbol{\sigma}_{\text{const}} + \lambda \boldsymbol{\sigma}_{\text{var}}, \tag{2}$$

where $\boldsymbol{\sigma}_{\text{const}}$ and σ_{var} are the stresses associated with $\boldsymbol{u}_{\text{const}}$ and $\boldsymbol{u}_{\text{var}}$, respectively. The variable displacement field $\boldsymbol{u}_{\text{var}}$ is obtained from a linear equilibrium solution based on the current tangent stiffness of the structure, while the constant component $\boldsymbol{u}_{\text{const}}$ remains unchanged until a new damage event is triggered.

A key feature of the Total formulation is that each damage event corresponds to a fully equilibrated structural configuration, regardless of the number of events that occurred in previous phases. This characteristic is essential for non-proportional problems, where internal forces generated by earlier actions, such as foundation settlement, significantly influence the response to subsequent loading. Within this framework, changes in stiffness and load path occur only through discrete, event-based updates, providing a consistent basis for tracking damage evolution across multiple loading stages.

2.2 *Event-driven damage and load scaling*

Damage evolution in the Total SLA framework follows an event-driven strategy. Loading progresses through the activation of discrete damage events rather than through predefined load or displacement increments. At each analysis step, the load factor is increased until the next interface integration point reaches its strength limit.

For a given structural state defined by the constant stress field $\boldsymbol{\sigma}_{\text{const}}$ and the variable stress field $\boldsymbol{\sigma}_{\text{var}}$, the critical load factor associated with a potential damage event is determined by enforcing the relevant failure criterion at the interface level.

The global damage event is defined by the minimum admissible value of the load factor over all interfaces and all damage modes. For each interface element i and damage mode k, the critical load factor is obtained as:

$$\lambda_{\text{crit}} = \min_{i,k}\left(\frac{f_{i,k} - \boldsymbol{\sigma}_{\text{const},\,i,k}}{\boldsymbol{\sigma}_{\text{var},\,i,k}}\right), \tag{3}$$

where $f_{i,k}$ is the current discrete strength threshold associated with that mode. Only positive values of λ are considered, ensuring that damage is triggered exclusively by load increases consistent with the prescribed loading direction.

It is noteworthy that settlement is applied as prescribed action and the overburden load remains constant throughout the analysis. The load factor λ_{crit} therefore scales only the variable pushover load.

This formulation ensures that damage activation is intrinsically linked to the failure mechanism at each step. No iterative equilibrium corrections or convergence tolerances are required. As a result, the resulting damage sequence reflects the evolving stress redistribution within the structure and naturally captures the interaction between different loading components under non-proportional conditions.

2.3 *Discrete constitutive law and state variables*

The nonlinear behavior of masonry is represented using zero-thickness interface elements, while masonry units are assumed linear elastic. All inelastic deformation is therefore concentrated at the interfaces.

At each interface, damage is described by discrete failure modes corresponding to tensile opening and shear sliding. Each mode is associated with an independent strength limit and stiffness branch. Continuous softening is approximated by a stepwise "saw-tooth" degradation scheme (Rots et al., 2008), in which stiffness and strength are reduced incrementally after each damage event.

Tensile damage represents crack opening across mortar joints or through unit splitting interfaces and governs the degradation of normal stiffness under opening conditions. Shear damage follows a frictional failure criterion and captures sliding along bed and head joints under combined normal and tangential stresses. Compressive crushing is not considered in this study, as its contribution is negligible for the investigated loading scenarios.

For each interface, damage modes are tracked independently. The current damage state acts as an index to the corresponding discrete stiffness and strength levels. This formulation ensures irreversible and path-dependent damage evolution without introducing continuous internal variables or iterative constitutive updates.

2.4 *Dual-stiffness strategy*

Non-proportional loading paths involving crack opening, closure, and re-opening can lead to numerical issues when damage is modeled through discrete stiffness reductions. To address these issues, a dual-stiffness strategy is adopted.

Two global stiffness matrices are maintained throughout the analysis. The tangent stiffness matrix represents the current damaged configuration and is used to compute the variable displacement field associated with the imposed loading direction. For interfaces experiencing tensile damage, the tangent normal stiffness is reduced to a small residual value, preventing tensile force transfer across open cracks.

A second stiffness matrix, referred to as the compressive stiffness, is used to evaluate internal forces and enforce global equilibrium at each damage event. In this matrix, interfaces remain able to transmit compressive forces even after tensile cracking, ensuring mechanical consistency during crack closure.

By separating displacement prediction from force equilibrium, the dual-stiffness strategy avoids numerical locking and artificial energy generation. This distinction is essential for non-proportional loading problems, such as settlement followed by lateral loading. Both stiffness matrices are updated only at discrete damage events, in accordance with the Total SLA formulation.

2.5 *Kinematic treatment of foundation settlement*

Foundation settlement is introduced as a kinematic loading phase defined by prescribed displacements. The settlement profile is formulated as a displacement vector and incorporated into the Total SLA framework as the variable loading component. Its magnitude is progressively scaled until the activation of the next damage event, in accordance with the event-driven strategy.

To track damage across multiple loading phases, two mode-dependent state variables are defined at each interface, namely S_t for tensile damage and S_s for shear damage. These variables evolve only at discrete damage events and record the cumulative damage associated with each failure mechanism. Each state variable acts as a pointer to pre-defined stiffness and strength levels, allowing interface properties to be updated without continuous constitutive evolution.

Damage accumulated during the settlement phase is directly inherited by subsequent loading stages. For example, interfaces cracked in tension during settlement enter the pushover phase with reduced stiffness and strength, affecting both tensile and shear response. State variables remain unchanged unless further damage is activated, preserving the structural memory and ensuring consistent damage evolution under non-proportional loading.

3 NUMERICAL PROGRAM

The numerical program is developed to investigate the load-path dependency of URM walls using the proposed Total SLA framework. The analyses follow a phased procedure that includes overburden loading, an optional settlement phase, and subsequent lateral pushover loading. This setup allows the influence of settlement-induced pre-damage on the later structural response to be evaluated in a controlled manner.

3.1 *Geometry and configurations*

Two wall configurations are considered. The first is a solid rectangular URM wall with dimensions of 990 × 1116 mm. The second configuration represents a wall with geometric discontinuity. It consists of a wall with overall dimensions of 3126 × 2700 mm and a central window opening of 794 × 1496 mm.

Both walls are modeled using a detailed micro-modeling approach. Brick units follow the standard Waal format with dimensions of 210 × 52 × 100 mm. Mortar joints and potential brick splitting planes are represented by zero-thickness interface elements. The geometric configurations and discretization are shown in Figure 1.

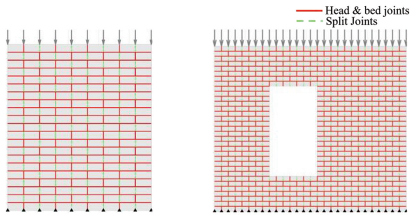

Figure 1. 2D micro-model of the URM walls subjected to overburden loading.

3.2 *Material parameters*

A consistent set of material and interface parameters is used in all simulations. The values are taken from

Table 1. Material properties of masonry components.

Masonry Units	Model	Parameters	Values	Units
Bricks	Linear Elastic	E_0	16.7	GPa
		ν_0	0.15	-
Head/Bed Joint	Tension	k_t	82	N/mm^3
		f_t	0.25	MPa
		G_f^I	0.018	N/mm
	Shear	k_s	36	N/mm^3
		c	0.35	MPa
		ϕ	30	∘
		G_f^{II}	0.125	N/mm
Split Joint	Tension	f_t	2	MPa
		G_f^I	0.08	N/mm

previous experimental studies (Raijmakers & Vermeltfoort 1992, Lourenço 1996) and are summarized in Table 1.

Brick units are modeled as linear elastic. All nonlinear behavior is concentrated in the interface elements representing mortar joints and potential brick cracks. These interfaces account for tensile cracking and shear sliding through discrete constitutive laws.

The progressive degradation of interface stiffness and strength is approximated using a discrete "sawtooth" scheme. The discretization factor p is set to 0.15 (Rots et al. 2008, Pari & Rots 2018). A schematic representation of this approach is shown in Figure 2.

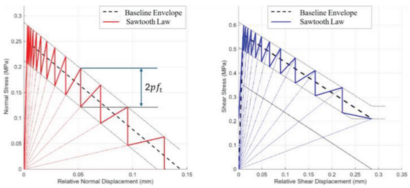

Figure 2. Stepwise degradation of interface stiffness and strength adopted in the Total SLA framework.

3.3 *Boundary condition and loading cases*

Three top boundary conditions are considered. In the *Free* configuration, the top of the wall is left unconstrained. In the *Cantilever* configuration, the top is modeled as a rigid beam that can translate and rotate. In the *Fixed* configuration, the top is modeled as a rigid beam that prevents rotation while allowing rigid-body translation.

An overburden pressure of 0.3 MPa is applied at the top boundary to represent gravity loads from upper stories. This load remains constant throughout the analysis. After the overburden phase, a monotonic lateral pushover load is applied at the top boundary.

Baseline pushover analyses are carried out for all three top boundary conditions. Analyses involving settlement-induced damage are limited to the free-top configuration in order to isolate the effects of settlement.

3.4 *Settlement scenarios*

Foundation settlement is introduced as a separate kinematic loading phase preceding the pushover analysis. Settlement is imposed through prescribed vertical displacements $u_{\text{target}}(x)$ applied to the bottom boundary nodes.

An asymmetric foundation settlement profile, with a maximum vertical displacement of 50 mm, is defined a priori and applied incrementally at the wall base. This allows damage to develop progressively during the settlement phase before lateral loading is applied.

Settlement-induced damage is investigated under free-top boundary conditions for both wall configurations. After the settlement phase, pushover loading is applied while preserving the accumulated damage state. In this way, the residual lateral capacity after settlement is evaluated consistently within the Total SLA framework.

4 NUMERICAL RESULTS

4.1 *Baseline pushover response without settlement*

The baseline pushover response of the walls without foundation settlement is first examined. Figures 3 and 4 compare the horizontal load–displacement curves for both wall configurations under the three top boundary conditions. It should be noted that the solid wall and the wall with opening have different dimensions and load-bearing areas, and thus, the force levels are discussed separately for each geometry.

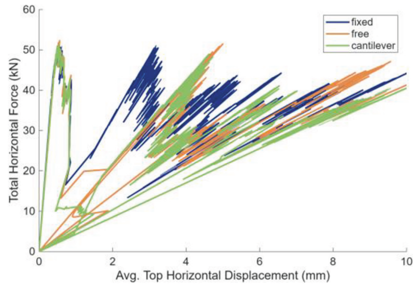

Figure 3. Pushover curves of the solid wall under three top boundary conditions.

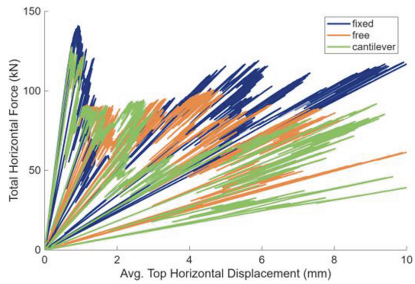

Figure 4. Pushover curves of the wall with opening under three top boundary conditions.

For both wall configurations, the initial elastic response is almost identical for all top boundary conditions. This indicates that, prior to cracking, the global stiffness is mainly governed by the masonry geometry and material properties and is only weakly influenced by the kinematic restraint at the top.

Differences between boundary conditions become apparent after the first interface cracking event. For the solid wall (Figure 3), the response is characterized by two distinct stages. After the first peak, a rapid reduction in stiffness and load-carrying capacity is observed, which is associated with the initiation of cracking and partial rocking of the wall.

This initial softening phase is similar for all boundary conditions. At larger displacements, however, the responses start to differ. The fixed-top configuration shows an earlier recovery of load-carrying capacity, reaching a relatively stable force level. This behavior indicates a faster re-engagement of frictional resistance after cracking. In contrast, the free-top and cantilever configurations experience more pronounced local sliding before strength recovery occurs. After this sliding-dominated phase, their responses converge toward a force level comparable to that of the fixed-top case. This suggests that, although the post-cracking mechanisms differ, frictional sliding along mortar joints governs the later-stage response of the solid wall under all boundary conditions.

For the wall with opening (Figure 4), the influence of top boundary conditions is more pronounced. The fixed-top configuration exhibits a larger strength drop immediately after cracking, which can be attributed to stress concentration around the opening combined with stronger kinematic restraint. At larger displacements, however, the fixed-top wall maintains a slightly higher overall load level. In contrast, the free-top and cantilever configurations show more extensive sliding, as also reflected in the corresponding damage patterns. As a result, their post-peak response stabilizes at a lower force level.

Moreover, the final damage distributions are summarized in Figures 5 and 6. For both wall geometries, damage localizes primarily along mortar joints, forming diagonal cracking bands consistent with combined tensile and shear deformation.

For the wall with opening (Figure 6), damage localizes earlier and more clearly around the opening corners. These regions act as stress concentrators and trigger early cracking, which limits the redistribution of internal forces. Once cracking initiates around the opening, the structural response rapidly

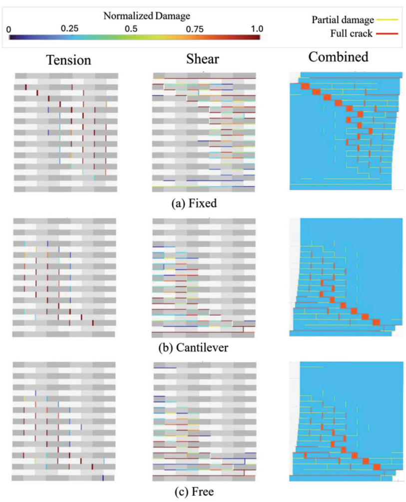

Figure 5. Final damage modes of the solid wall with three top boundary conditions.

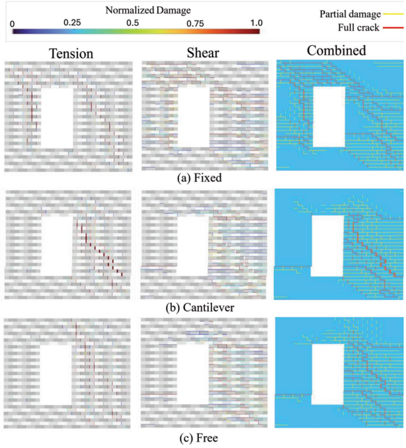

Figure 6. Final damage modes of the wall with opening with three top boundary conditions.

transitions toward sliding mechanisms, particularly in configurations with reduced top restraint. This explains the sharper post-peak degradation observed in Figure 4 for the free-top and cantilever cases.

4.2 *Settlement-induced damage & sequential pushover response*

The structural response under foundation settlement is analyzed, where only free-top boundary is adopted. The pre-damaged walls are further simulated under subsequent pushover loading. The damage states obtained at the end of the settlement phase and the subsequent pushover phase are shown in Figures 7 and 8.

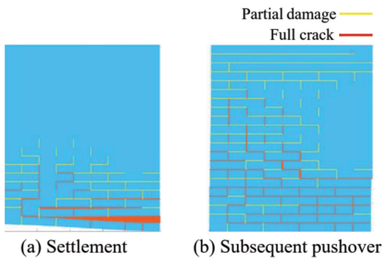

Figure 7. Final damage pattern for the solid wall after settlement and subsequent pushover.

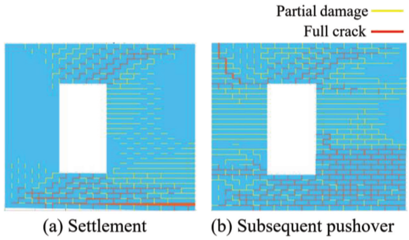

Figure 8. Final damage pattern for the wall with opening after settlement and subsequent pushover.

For both wall configurations, the settlement phase activates cracking and sliding at the interface level before any lateral load is applied. These damage patterns are not removed or redistributed during the pushover phase. Instead, they continue to govern the subsequent damage evolution.

In the solid wall (Figure 7), settlement induces localized cracking and sliding near the base. During the following pushover phase, these pre-existing damage zones extend and connect, leading to earlier activation of dominant sliding paths. In the wall with opening (Figure 8), settlement-induced cracks concentrate near the base and around the opening corners. During pushover loading, damage propagates from these zones, confirming that the failure mechanism is strongly influenced by the inherited damage state.

Overall, the combined settlement–pushover analyses show that the lateral response does not develop independently of the settlement phase. Instead, pushover loading amplifies and extends the damage patterns initiated during settlement, highlighting the path-dependent nature of the response.

4.3 *Influence of settlement-induced pre-damage on pushover capacity*

The influence of settlement-induced pre-damage on the lateral response is quantified by comparing pushover curves obtained with and without prior settlement. Figures 9 and 10 present the results for the solid wall and the wall with opening, respectively.

For the solid wall (Figure 9), settlement leads to a clear reduction in peak lateral capacity. stiffness degradation starts at smaller displacement levels compared to the reference pushover without settlement. This indicates that settlement-induced damage reduces both the effective stiffness and the available strength, even when the overall damage pattern remains relatively localized.

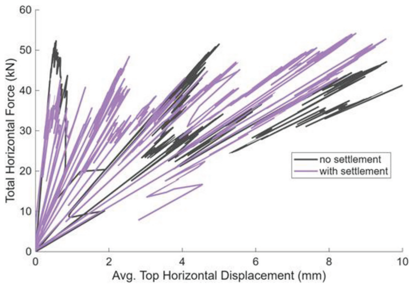

Figure 9. Pushover response of the solid wall with vs. without settlement.

The effect of settlement is more pronounced for the wall with opening (Figure 10). Both the initial stiffness and the peak capacity are reduced after settlement. The response shows earlier softening and a more rapid strength degradation. This behavior reflects the interaction between settlement-induced cracking and stress concentrations around the opening, which accelerates damage localization and limits load redistribution.

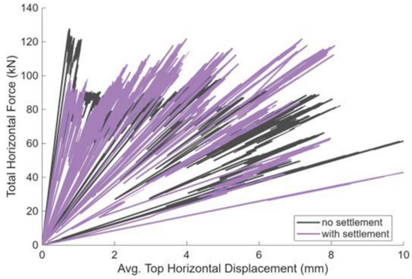

Figure 10. Pushover response of the wall with opening with vs. without settlement.

These results confirm that settlement-induced damage cannot be represented simply by a reduction factor applied to the pushover curve. Instead, the entire response evolves from a modified damage state, leading to changes in stiffness, strength, and failure mechanism.

5 DISCUSSION

The numerical results highlight the strong influence of load-path dependency on the structural response of URM walls. Both boundary conditions and foundation settlement play a key role in determining damage localization, stiffness degradation, and residual load-carrying capacity.

Top boundary conditions mainly affect the post-cracking response. While the initial elastic stiffness is almost unaffected, clear differences emerge once interface cracking initiates. Fixed-top conditions delay the development of dominant sliding mechanisms by providing additional kinematic restraint. As a result, stiffness degradation occurs more gradually, and higher force levels are maintained during the later stages of loading. In contrast, free-top and cantilever conditions allow earlier sliding along mortar joints, leading to faster strength reduction after cracking. The similarity observed between these two cases indicates that rotational restraint provided by the cantilever condition becomes ineffective once cracking and sliding dominate the response.

Openings introduce stress concentrations and interrupt load-transfer paths, which promotes early damage localization around opening corners. Once cracking develops in these regions, the ability of the wall to redistribute internal forces is reduced. Consequently, differences in post-peak response between boundary conditions become more pronounced in walls with openings, even though the elastic response remains similar.

Foundation settlement introduces irreversible pre-damage that significantly influences the subsequent pushover response. Settlement-induced cracking and sliding affect the stiffness distribution and the deformation paths during lateral loading. When pushover loading follows, the structural response evolves from this pre-damaged state. This results in reduced stiffness, lower peak capacity, and earlier softening compared to walls without prior settlement. These effects are particularly evident in walls with openings, where settlement-induced damage interacts with existing stress concentration zones.

While the prescribed displacement approach adopted in this study allows precise control of the imposed settlement profile, it introduces a kinematic constraint at the soil–structure interface. As a result, the masonry wall is forced to follow the imposed deformation pattern, which may promote localized stress concentrations and early activation of interface cracking near the base. This effect is particularly relevant in regions where settlement gradients are steep.

In real conditions, the supporting soil exhibits finite compliance, and soil–structure interaction effects allow the superstructure to partially bridge over the settlement trough through the mobilization of arching mechanisms. Such mechanisms may reduce local deformation demands and delay damage activation compared to a fully kinematic boundary condition.

For future investigations, a more physically representative strategy would be to introduce settlement through a compliance-driven formulation. In this approach, spatial variations of foundation stiffness would be prescribed instead of nodal displacements, allowing settlement to develop naturally under gravitational loading. This force-controlled setting would avoid overly restrictive kinematic constraints at the base and is expected to provide a more realistic representation of settlement-induced pre-damage, as well as a more consistent initial state for subsequent lateral or seismic assessments.

From a modeling perspective, the results confirm that proportional pushover analyses are not sufficient to represent the response of masonry structures subjected to sequential actions. The observed changes in stiffness, strength, and failure mechanism cannot be captured by simple reduction factors applied to monotonic pushover curves. Instead, the response depends on the order and nature of the applied loads.

The Total Sequentially Linear Analysis framework adopted in this study provides a consistent way to address this problem. By enforcing global equilibrium at each damage event and allowing damage states to be inherited across loading phases, the framework captures the accumulation and interaction of damage under non-proportional loading. This makes it well suited for studying masonry structures subjected to combined settlement and lateral loading within a simplified yet mechanically transparent modeling approach.

6 CONCLUSIONS

This study investigated the response of unreinforced masonry (URM) walls under non-proportional loading conditions using a Total SLA framework. Based on the numerical results, the following conclusions can be drawn:

Top boundary conditions have a limited influence on the initial elastic response of URM walls but significantly affect the post-cracking behavior. Differences mainly arise in the softening phase, where kinematic restraint controls the transition between cracking, sliding, and frictional re-engagement.

Walls with openings exhibit a stronger sensitivity to boundary conditions. Stress concentrations around openings lead to earlier damage localization and limit force redistribution, resulting in larger differences in peak capacity and residual strength between boundary configurations.

Foundation settlement causes irreversible pre-damage that remarkably reduces stiffness and lateral load-carrying capacity during subsequent pushover loading.

The structural response of URM walls is strongly load-path dependent. Sequential settlement–pushover analyses produce different stiffness degradation patterns and failure mechanisms compared to monotonic pushover analyses.

The proposed Total SLA framework provides a robust tool for modeling non-proportional loading histories. The framework captures the interaction between settlement-induced damage and lateral response within a simplified modeling strategy.

REFERENCES

Amorosi, A. et al. 2014. Tunnelling-induced deformation and damage on historical masonry structures. *Géotechnique* 64(2): 118–130.

DeJong, M.J. 2008. Sequentially linear analysis of fracture under non-proportional loading. *Engineering Fracture Mechanics* 75: 5042–5056.

Giardina, G. et al. 2012. Experimental analysis of a masonry façade subject to tunnelling-induced settlement. *Engineering Structures* 45: 421–434.

Korswagen, P.A. et al. 2022. Fragility curves for light damage of clay masonry walls subjected to seismic vibrations. *Bulletin of Earthquake Engineering* 20: 6193–6227.

Koutras, A.A. & Shing, P.B. 2021. Finite-element modeling of the seismic response of reinforced masonry wall structures. *Earthquake Engineering & Structural Dynamics* 50(4): 1125–1146.

Lourenço, P.B. 1996. Computational strategies for masonry structures. PhD thesis, *Delft University of Technology*, Delft.

Massart, T.J. 2007. Structural Damage Analysis of Masonry Walls using Computational Homogenization. *International Journal of Damage Mechanics* 16(2): 199–226.

Pari, M. & Rots, J.G. 2018. Non-proportional loading for 3-D stress situations in Sequentially Linear Analysis. *International Journal for Numerical Methods in Engineering* 19(6): 506–531.

Pulatsu, B. et al. 2020. Simulation of the in-plane structural behavior of unreinforced masonry walls and buildings using DEM. *Structures* 27: 2274–2287.

Raijmakers, T. & Vermeltfoort, A.T. 1992. Deformation controlled tests in masonry shear walls. Report B-92-1156, *TNO-Bouw*, Delft.

Rots, J.G. &. Invernizzi, S. 2004. Regularized sequentially linear saw-tooth softening model. *International Journal for Numerical and Analytical Methods in Geomechanics* 28 (7-8): 821–856.

Rots, J.G. et al. 2008. Robust modeling of RC structures with an “event-by-event” strategy. *Engineering Fracture Mechanics* 75(3-4): 590–614.